

Growth mechanism of the Si $\langle 110 \rangle$ faceted dendrite

K. Fujiwara,* H. Fukuda, N. Usami, K. Nakajima, and S. Uda

Institute for Materials Research (IMR), Tohoku University, Katahira 2-1-1, Aoba-ku, Sendai 980-8577, Japan

(Received 20 February 2010; published 14 June 2010)

The growth mechanism of the Si $\langle 110 \rangle$ faceted dendrite was studied using an *in situ* observation technique. We directly observed the growth process of Si faceted dendrites from Si melts. It was found that the shape of the $\langle 110 \rangle$ faceted dendrite during growth is markedly different from that of the $\langle 112 \rangle$ faceted dendrite; the tip of the $\langle 110 \rangle$ faceted dendrite is narrow while that of the $\langle 112 \rangle$ faceted dendrite is wide. We present a scheme for the growth shapes of the faceted dendrites based on the experimental evidences.

DOI: 10.1103/PhysRevB.81.224106

PACS number(s): 81.10.Aj, 64.70.dg, 68.35.bg, 81.10.Fq

I. INTRODUCTION

Dendritic growth is a widespread phenomenon that appears during crystallization from a liquid or vapor phase in almost all types of materials. The growth behaviors of dendrites of nonfaceted materials, typified by metals and alloys, have been extensively investigated by experiments and theoretically,^{1–3} and the shape of dendrites during growth has been replicated by phase-field simulations.^{4–6} The large number of studies on the dendritic growth of nonfaceted materials are well summarized in Ref. 7. However, the growth behaviors of dendrites of faceted materials such as Si and Ge are still unclear owing to the lack of experimental investigation.

It is known that twin-related dendrites of Si or Ge, so-called “faceted dendrites,” have unique crystal structures.^{8–20} The surface of these dendrites is bounded by $\{111\}$ habit planes and at least two parallel twins exist at the center of each dendrite. It was also shown that the preferential growth directions of Si faceted dendrites are $\langle 112 \rangle$ and $\langle 110 \rangle$.¹⁸ Such features of faceted dendrites can be applied in technologies for growing thin Si ribbon crystals^{13,14} and polycrystalline Si ingots^{21,22} for solar cells. A growth mechanism for the dendrite preferentially grown along the $\langle 112 \rangle$ direction, hereafter referred to as a $\langle 112 \rangle$ dendrite, was first proposed in 1960.^{10,11} Recently, we proposed a scheme for the growth shape of the $\langle 112 \rangle$ dendrite based on experimental results of the growth behavior of $\langle 112 \rangle$ dendrites.²⁰ That fully explains the shape of the $\langle 112 \rangle$ dendrite during growth. On the other hand, the experimental investigation of the $\langle 110 \rangle$ dendrite has been very limited. Nagashio and Kuribayashi¹⁸ analyzed the crystallographic orientation of Si faceted dendrites after crystallization from undercooled melts and showed that the $\langle 110 \rangle$ dendrite appeared at ΔT (undercooling) < 100 K. However, the growth process of the $\langle 110 \rangle$ dendrite has not been investigated in detail, and thus the growth behavior of the $\langle 110 \rangle$ dendrite has not yet been clarified.

In this study, we succeeded in directly observing the growth process of a $\langle 110 \rangle$ dendrite. A difference in the shape between the $\langle 110 \rangle$ dendrite and the $\langle 112 \rangle$ dendrite during growth was clearly observed. We present a scheme for the growth shape of the $\langle 110 \rangle$ dendrite based on our experimental results.

II. EXPERIMENTAL DETAILS

We used an *in situ* observation system, which consisted of a furnace and a microscope.^{20,23} The experimental procedure

is illustrated in Fig. 1(a). An orientation-controlled Si sheet crystal was prepared, as shown in Fig. 1(a). The sheet crystal was set inside the furnace. Then, the furnace was filled with ultrahigh-purity argon gas. The sample was carefully heated in such a way that an unmelted part remained, which played the role of a $\langle 110 \rangle$ seed. Then the sample was cooled rapidly to promote crystallization from the seed. In this way, we were able to observe the crystal-melt interface growing along the $\langle 110 \rangle$ direction from the $\langle 111 \rangle$ direction, as shown in Fig. 1(b). The $\langle 110 \rangle$ growth interface had a zigzag shape because $\{111\}$ facet faces appeared on the growth surface. The equilibrium shape of a Si crystal observed from the $\langle 111 \rangle$ direction is illustrated in Fig. 1(b). We can confirm that the crystal grows along the $\langle 110 \rangle$ direction from the angle between the facet faces on the interface. Images of the sample during melting and crystallization were recorded on a videotape. After crystallization, the crystallographic orientation was analyzed by the electron backscattering diffraction pattern (EBSP) method.

III. RESULTS AND DISCUSSION

Figure 2 shows the typical growth behavior of a Si crystal growing in the $\langle 110 \rangle$ direction. During the crystallization,

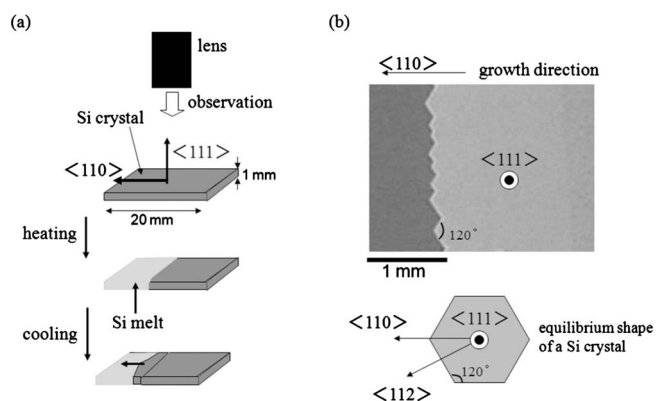


FIG. 1. (a) Experimental procedure for observing the growth behavior of a Si crystal growing in the $\langle 110 \rangle$ direction. (b) Example of a Si crystal-melt interface growing in the $\langle 110 \rangle$ direction observed from the $\langle 111 \rangle$ direction. The equilibrium form of the Si crystal is schematically shown. The facet shape of the crystal-melt interface coincides with the equilibrium form.

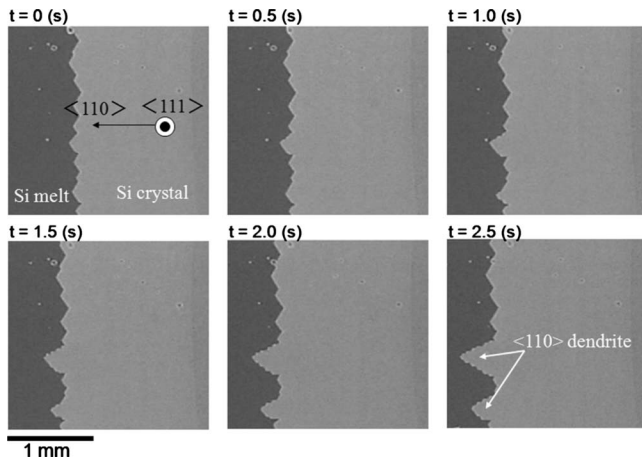


FIG. 2. Typical growth behavior of a Si crystal growing in the $\langle 110 \rangle$ direction. Dendrite growth appears at a part of the faceted interface. The dendrites preferentially grow in the $\langle 110 \rangle$ direction. The dendrites grow faster than the rest of the crystal.

dendritic growth was initiated at a part of the faceted interface. It was found that the dendrite preferentially grew in the $\langle 110 \rangle$ direction and that it grew faster than the rest of the crystal. For comparison, the growth process of the $\langle 112 \rangle$ dendrite is shown in Fig. 3, the behavior of which we reported in detail in Ref. 20. The experimental procedure followed to obtain the sample shown in Fig. 3 was similar to that for the sample shown in Fig. 2; the Si crystal grew from the $\langle 110 \rangle$ seed. From Fig. 3, it was found that the rapid growth direction of the dendrite is the $\langle 112 \rangle$ direction upon considering the orientation relationship illustrated in Fig. 1(b). The shape of the $\langle 112 \rangle$ dendrite during growth, shown in Fig. 3, is similar to that in the previous report.²⁰ Note that the shape of the tip of the growing dendrite is markedly different between

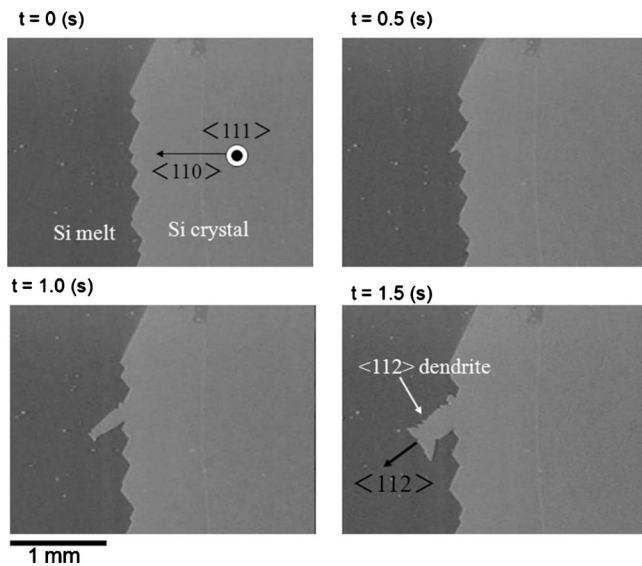


FIG. 3. Growth behavior of a Si $\langle 112 \rangle$ dendrite. The experimental procedure followed to obtain this sample was similar to that for the sample in Fig. 2. Note that the dendrite shape during growth is markedly different between the $\langle 112 \rangle$ dendrite and the $\langle 110 \rangle$ dendrite shown in Fig. 2.

the $\langle 110 \rangle$ dendrite and the $\langle 112 \rangle$ dendrite. While the tip of the $\langle 112 \rangle$ dendrite becomes wider during growth, that of the $\langle 110 \rangle$ dendrite remains narrow during growth. We considered that there were two possible causes of the difference in the shape of the dendrites: (1) their structural features are different and (2) their growth mechanisms are different. Regarding the former, it is well known that the $\langle 112 \rangle$ dendrite is bounded by $\{111\}$ planes and that it contains parallel twins.^{8–20} To investigate the structural features of the $\langle 110 \rangle$ dendrite, we analyzed its crystallographic orientation (Fig. 4). The color in the orientation map corresponds to the color in the stereotype triangle. First, the orientation of the top surface of the dendrite was investigated [Fig. 4(a)]. It was confirmed that the upper surface of the dendrite is $\{111\}$ (colored blue). Next, we cut the sample perpendicular to the direction of preferential growth and the orientation was analyzed [Fig. 4(b)]. It was found that the dendrite preferentially grew along the $\langle 110 \rangle$ direction (colored green), and that there are parallel twins as shown by the red lines in Fig. 4(b). This structural feature is similar to that of the $\langle 112 \rangle$ dendrite. Thus, we found that the structural features of the $\langle 110 \rangle$ and $\langle 112 \rangle$ dendrites are the same: their surfaces are bounded by $\{111\}$ habit planes and they contain parallel twins. Therefore, the difference in the shape during growth is attributed to a difference in the growth mechanism. We have already presented a scheme for the growth shape of the $\langle 112 \rangle$ dendrite, in which its wide tip is fully explained.²⁰ On the other hand, the growth mechanism of the $\langle 110 \rangle$ dendrite has not been proposed yet because its growth process was observed in this study. Thus, we next consider why the growth shape is different between the $\langle 110 \rangle$ dendrite and the $\langle 112 \rangle$ dendrite.

First, we review the scheme for the growth shape of the $\langle 112 \rangle$ dendrite in Fig. 5, which we presented in Ref. 20. The top view of a growing dendrite is also illustrated in Fig. 5. Figure 5(a) shows the equilibrium form of the Si crystal with two parallel twins. The crystal is bounded by $\{111\}$ habit planes and two parallel twin planes exist parallel to the $\langle 111 \rangle$ upper surface. In the explanation, the two twins are distinguished by labeling them twin₁ and twin₂. Here we consider the situation that the crystal is growing only in one direction, the $\langle 112 \rangle$ direction, for the sake of simplicity. A reentrant corner with an external angle of 141° (type I) appears at the growth surface only at twin₁. Nucleation more readily occurs at the reentrant corner than at $\{111\}$ flat surfaces,^{8–11,18} and thus the rapid growth occurs there. In this growth mechanism, it is considered that a triangular corner with an angle of 60° is formed at the growth tip of the dendrite owing to the rapid growth at the reentrant type I corner, as shown in Fig. 5(b). This is the major difference from the previous growth mechanism of the $\langle 112 \rangle$ dendrite presented by Hamilton and Seidensticker.¹⁰ In their explanation, it was considered that the formation of a triangular corner disturbed the continuous growth of the dendrite because the reentrant type I corner was disappeared.¹⁰ However, we confirmed the formation of a triangular corner at the tip of the $\langle 112 \rangle$ dendrite by *in situ* observations.²⁰ Crystal growth can continue on the $\{111\}$ flat surface although the rapid growth is inhibited owing to the disappearance of the type I corner [Figs. 5(b) and 5(c)]. After the propagation of the crystal, two type I corners are newly formed on the growth surface at twin₂ [Fig. 5(c)].

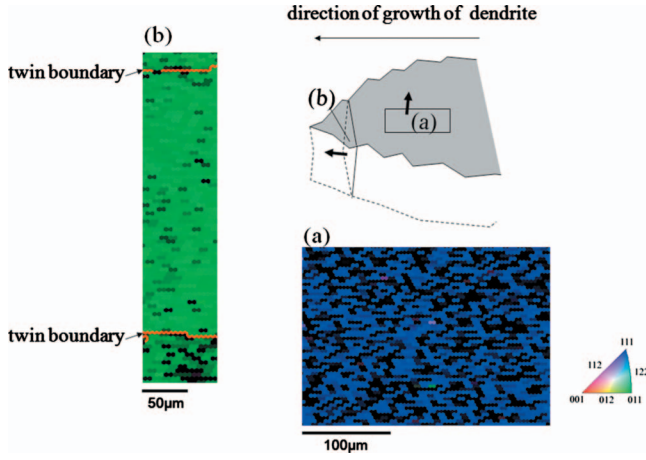


FIG. 4. (Color) Results of EBSD analysis of the $\langle 110 \rangle$ dendrite. (a) Orientation map of the top surface of the dendrite. It was confirmed that the surface is $\{111\}$. (b) Orientation map of the plane cut perpendicular to the preferential growth direction. We confirmed that the dendrite preferentially grows in the $\langle 110 \rangle$ direction as well as the existence of two parallel twins shown by red lines.

Thus, rapid growth occurs there again and triangular corners with an angle of 60° are formed in the same manner as before [Fig. 5(d)]. Crystal growth is promoted on the $\{111\}$ flat surface, leading to the formation of a new reentrant type I corner at twin_1 [Fig. 5(e)] and the rapid growth occurs again [Fig. 5(f)]. The faceted dendrite continues to grow by the repetition of the same processes. Note that the tip of the dendrite becomes wider with increasing crystal growth. The shape obtained by this mechanism agrees with the shape experimentally observed in Fig. 3.

Next, we consider a growth of the $\langle 110 \rangle$ dendrite in Fig. 6. Two parallel twins are contained in the $\langle 110 \rangle$ dendrite, as confirmed in Fig. 4. Thus, the initial shape of the crystal should be the same as that shown in Fig. 5(a). This means that the elementary process for the growth of the $\langle 110 \rangle$ dendrite should be the same as that of the $\langle 112 \rangle$ dendrite. Here, we consider that the crystal only grows along the $\langle 110 \rangle$ direction, similarly to the result of our experiment shown in Fig. 2. The top view shown in Fig. 6(a) corresponds to the shape of the faceted interface observed in Fig. 2. It is found that the type I corners exist at both twin_1 and twin_2 [Fig.

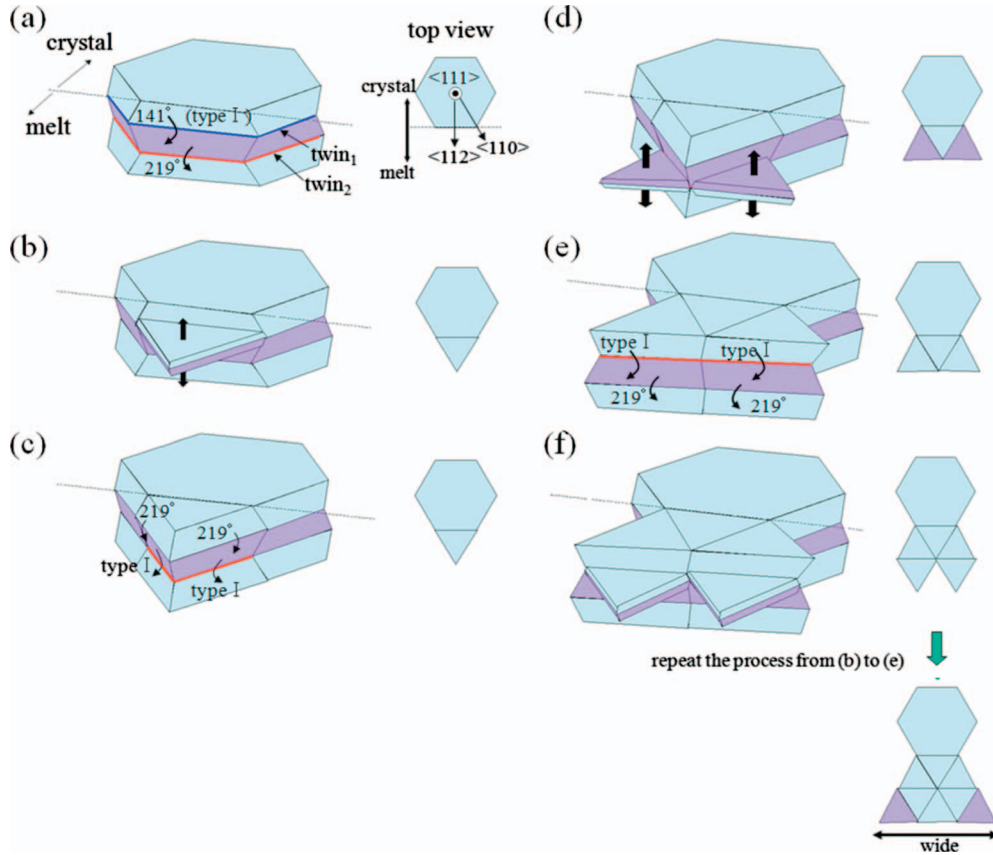


FIG. 5. (Color) Schematic images of the growth of a Si $\langle 112 \rangle$ dendrite, which was previously proposed (Ref. 20). (a) Equilibrium form of a crystal with two twins, which is bounded by $\{111\}$ habit planes. It is considered that the crystal is growing only in the $\langle 112 \rangle$ direction for the sake of simplicity. A reentrant corner of angle 141° (type I) appears at the growth surface only at twin_1 . (b) A triangular corner is formed owing to the rapid growth at the type I corner at twin_1 . (c) Crystal growth can continue on the $\{111\}$ flat surface, although the rapid growth is inhibited because of the disappearance of the type I corner. When the triangular crystal propagates across twin_2 , two type I corners are newly formed at twin_2 . (d) Rapid growth occurs at the two type I corners again and a triangular corner is formed. (e) After propagation of the crystal, a type I corner is formed at twin_1 . (f) Rapid growth occurs at a type I corner. The faceted dendrite continues to grow along the $\langle 112 \rangle$ direction by repeating the process from (b) to (f). Note that the tip of the $\langle 112 \rangle$ dendrite becomes wider with progressing crystal growth, which is in agreement with the result of the *in situ* observation shown in Fig. 3.

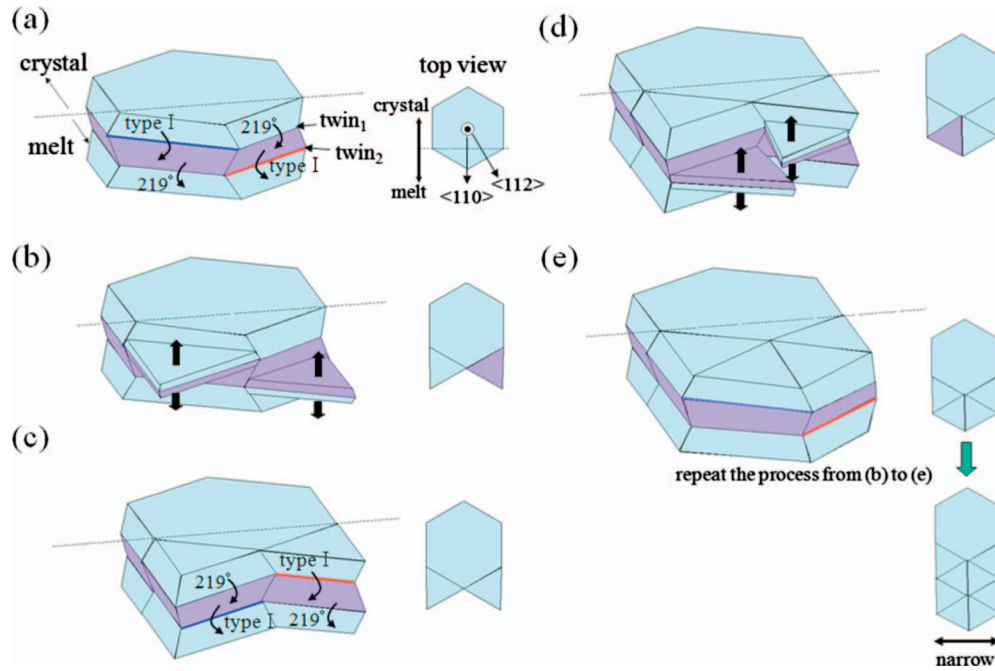


FIG. 6. (Color) A scheme for the growth shape of the $\langle 110 \rangle$ dendrite. (a) Equilibrium form of a crystal with two twins, which is similar to that shown in Fig. 5(a). It is considered that the crystal is growing only in the $\langle 110 \rangle$ direction. Reentrant type I corners appear at both twin₁ and twin₂. This is markedly different from the growth of the $\langle 112 \rangle$ dendrite. (b) Triangular corners are formed owing to the rapid growth at both twins. (c) Crystal growth can continue on the $\{111\}$ flat surface. When the triangular crystals propagate across another twin, two type I corners are newly formed at both twins. (d) Rapid growth occurs at the two type I corners again and triangular corner is formed. (e) After propagation of the triangular crystals, type I corners are formed at the both twins. The faceted dendrite continues to grow along the $\langle 110 \rangle$ direction by repeating the process from (b) to (e). In these growth processes, the tip of the dendrite remains narrow during crystal growth, which can explain the shape of the $\langle 110 \rangle$ dendrite during growth shown in Fig. 2.

6(a)]. Therefore, rapid growth should occur at these two type I corners simultaneously [Fig. 6(b)]. This is a major difference from the case of the $\langle 112 \rangle$ dendrite, in which the type I corner alternately appears at each twin. The later growth processes are similar to those of the $\langle 112 \rangle$ dendrite. The rapid growth at the type I corners leads to the formation of triangular corners [Fig. 6(b)]. Although the rapid growth is inhibited after the formation of triangular corners, the crystal continuously grows on the $\{111\}$ flat surface [Figs. 6(b) and 6(c)]. Again, the type I corners appear at both twins [Fig. 6(c)] and rapid growth occurs there [Fig. 6(d)]. When the triangular crystals propagate across the other twin, two type I corners appear [Fig. 6(e)]. It should be emphasized that the type I corners always appear at both twins simultaneously in this process. Note that the tip of the dendrite remains narrow during crystal growth. Thus, we can explain the shape of the $\langle 110 \rangle$ dendrite during growth, shown in Fig. 2, by this mechanism.

It was clarified that there is no structural difference between the $\langle 110 \rangle$ dendrite and the $\langle 112 \rangle$ dendrite but the den-

drite shape during crystallization is different in terms of its dependence on the preferential growth direction as shown in Figs. 2 and 3. We can explain the difference by the scheme for the growth shapes of the faceted dendrites presented in Figs. 5 and 6.

IV. CONCLUSIONS

We investigated the growth behavior of Si faceted dendrites preferentially grown in the $\langle 110 \rangle$ and $\langle 112 \rangle$ directions by *in situ* observations. It was directly proved that the shape of the dendrite during growth is determined by the preferential growth direction. We present a scheme for the growth shapes of the faceted dendrites. That fully explains the shape of the dendrites during growth.

ACKNOWLEDGMENTS

This work was partially supported by a Grant-in-Aid for Scientific Research No. 21686001 from the Ministry of Education, Culture, Sports, Science and Technology of Japan. K.F. would like to thank A. Kudo for fruitful talks.

*Corresponding author. FAX: +81-22-215-2101; kozo@imr.tohoku.ac.jp

- ¹W. Kurz and D. J. Fisher, *Fundamentals of Solidification*, 4th rev. ed. (Trans Tech, Switzerland, 1998), Chap. 4.
- ²M. C. Flemings, *Solidification Processing* (McGraw-Hill, New York, 1974), Chap. 3, p. 6.
- ³Y. Saito, *Statistical Physics of Crystal Growth* (World Scientific, Singapore, 1996), Chap. 4.
- ⁴R. Kobayashi, *Physica D* **63**, 410 (1993).
- ⁵J. Bragard, A. Karma, Y. H. Lee, and M. Plapp, *Interface Sci.* **10**, 121 (2002).
- ⁶T. Haxhimali, A. Karma, F. Gonzales, and M. Rappaz, *Nature Mater.* **5**, 660 (2006).
- ⁷M. Asta, C. Beckermann, A. Karma, W. Kurz, R. Napolitano, M. Plapp, G. Purdy, M. Rappaz, and R. Trivedi, *Acta Mater.* **57**, 941 (2009).
- ⁸E. Billig, *Proc. R. Soc. London, Ser. A* **229**, 346 (1955).
- ⁹A. I. Bennett and R. L. Longini, *Phys. Rev.* **116**, 53 (1959).
- ¹⁰D. R. Hamilton and R. G. Seidensticker, *J. Appl. Phys.* **31**, 1165 (1960).
- ¹¹R. S. Wagner, *Acta Metall.* **8**, 57 (1960).
- ¹²N. Albon and A. E. Owen, *J. Phys. Chem. Solids* **24**, 899 (1963).
- ¹³S. O'Hara and A. I. Bennett, *J. Appl. Phys.* **35**, 686 (1964).
- ¹⁴D. L. Barrett, E. H. Myers, D. R. Hamilton, and A. I. Bennett, *J. Electrochem. Soc.* **118**, 952 (1971).
- ¹⁵C. F. Lau and H. W. Kui, *Acta Metall. Mater.* **39**, 323 (1991).
- ¹⁶D. Li and D. M. Herlach, *Phys. Rev. Lett.* **77**, 1801 (1996).
- ¹⁷T. Aoyama, Y. Takamura, and K. Kuribayashi, *Metall. Mater. Trans. A* **30**, 1333 (1999).
- ¹⁸K. Nagashio and K. Kuribayashi, *Acta Mater.* **53**, 3021 (2005).
- ¹⁹K. Fujiwara, K. Maeda, N. Usami, G. Sazaki, Y. Nose, and K. Nakajima, *Scr. Mater.* **57**, 81 (2007).
- ²⁰K. Fujiwara, K. Maeda, N. Usami, and K. Nakajima, *Phys. Rev. Lett.* **101**, 055503 (2008).
- ²¹K. Fujiwara, W. Pan, N. Usami, K. Sawada, M. Tokairin, Y. Nose, A. Nomura, T. Shishido, and K. Nakajima, *Acta Mater.* **54**, 3191 (2006).
- ²²T. Y. Wang, S. L. Hsu, C. C. Fei, K. M. Yei, W. C. Hsu, and C. W. Lan, *J. Cryst. Growth* **311**, 263 (2009).
- ²³M. Tokairin, K. Fujiwara, K. Kutsukake, N. Usami, and K. Nakajima, *Phys. Rev. B* **80**, 174108 (2009).